A01-34482

AIAA 2001–3846

Combustion Instabilities in Swirling Flows

C. Stone and S. Menon
School of Aerospace Engineering
Georgia Inst. of Technology
Atlanta, Georgia, USA 30332
cstone@cc.gatech.edu, suresh.menon@ae.gatech.edu
http://www.ccl.gatech.edu

37th AIAA/ASME/SAE/ASEE
Joint Propulsion Conference
July 8-11, 2001 / Salt Lake City, Utah

Combustion Instabilities in Swirling Flows

C. Stone*and S. Menon†
School of Aerospace Engineering
Georgia Inst. of Technology
Atlanta, Georgia, USA 30332
cstone@cc.gatech.edu, suresh.menon@ae.gatech.edu
http://www.ccl.gatech.edu

Large-Eddy Simulation (LES) methodology has been used to model combustion dynamics in a realistic swirling flow dump combustor. Two important design parameters, velocity swirl number (S) and fuel equivalence ratio (Φ), are parametrically altered to investigate their relative impact on the dynamics. A premixed flamelet model is employed to capture the interaction of the unsteady flame-front with local velocity fluctuations. It has been observed that higher swirling velocity profiles, those large enough to induce vortex break-down, substantially reduce pressure (over 6 dB reduction) and flame-front oscillations. In addition to swirl-vane angle effects, pressure amplitudes are shown to increase in the lean limit.

1 Introduction

Due to increasingly stringent emission regulations, clean burning, low NO_x combustion devices are in high demand. To achieve the desired emissions levels, modern combustion devices are designed to operate in the lean limit. The lower associated combustion temperatures result in suppression of thermal NO_x formation (Zeldovich thermal NO_x mechanism). However, as the equivalence ratio approaches the Lean-Blowout limit (LBO), the sensitivity to small perturbations in fuel concentration, flow velocity, temperature, and pressure increase due to the strong dependence of flame speed on local fuel content. Under certain conditions, these fluctuations can become self exciting and amplified, resulting in high-amplitude pressure oscillations. Structural fatigue, increased combustor core noise or possible even system failure could result if these oscillations are not positively controlled and attenuated.

At the heart of combustion dynamics is the coupling between heat release, velocity, and pressure oscillations in the combustor. Accurate prediction of the effects of such coupling is especially difficult due to the unsteadiness of the driving processes (e.g., fuel injection) and the highly nonlinear behavior of the interactions between turbulent mixing, acoustic wave propagation, and unsteady heat release. Large-scale flow structures play a key role in the coupling process by controlling the mixing of the essential ingredients of combustion: oxidizer, fuel, and heat.

Active control of combustion driven instabilities has been demonstrated through several means. Secondary fuel modulation has been demonstrated by Zinn and Neumeier.[1] Active flow control has been investigated by Paschereit *et al.*.[2,3] Passive control using sudden expansions or bluff-bodies has also been conducted but these studies predominantly focused upon axisymmetric flow instability, characteristic of non-swirling flows.

Swirl stabilized combustion is quite common in gas turbine combustors; however, it has been reported by Sivasegaram and Whitelaw[4] that swirl may drive instabilities in suddenly expanded flows. Unlike predominantly two-dimensional flows, azimuthal instability modes may be important in highly swirling flows. Swirl is often used as a flame stabilizing mechanism due to Vortex-Breakdown phenomena (i.e., axial flow-reversal). Vortex-Breakdown has a two-fold mechanism for flame stabilization: low axial velocities and preheating through recirculated product gas. Swirl stabilized combustion has been experimentally studied in the past and extensively reviewed by Lilley[5] and Syred.[6] More recently, experimental and numerical studies have been conducted on highly swirling combustion flows.[7,8] Non-reacting swirling flows through sudden expansions has been experimentally investigated by Dellenback *et al.*[9]

In order to control combustion instabilities, it is vital to understand the large-scale dynamics of these complex, turbulent flows. However, the harsh conditions inside the combustion system make experimental studies difficult and expensive. By accurately simulating the governing fluid physics, numerical modeling of such systems can lead to a more detailed understanding of the combustion processes.

The design of clean-burning combustion devices, both power-generation and propulsion, is extremely difficult and costly due to the previously mentioned sensitivity in the lean limit. Integrating high accuracy, time-dependent simulation tools, such as Large-Eddy Simulations (LES), into the design cycle can decrease experimental costs. For such a numerical tool to be effective, it must give sufficiently accurate results in

*Student Member, AIAA
†Associate Fellow, AIAA

a relatively short time-frame. To this end, this study will focus on the effects of various design parameters on the stability of the combustion device using LES methodology.

2 Numerical Model

The LES equations of motion are solved on a three dimensional, boundary-conforming grid using a finite volume scheme.[10] For brevity, the LES equations and numerical details are withheld but can be found elsewhere.[11] No-slip, adiabatic wall conditions conditions are used with non-reflecting inflow/outflow boundary conditions following Poinsot and Lele.[12] Clustering is employed near walls and in shear layer region to better resolve large scale fluctuations.

To increase simulation turn-around time, the computational domain is evenly distributed in parallel using the Message-Passing Interface (MPI) standard. An advantage of the explicit scheme used here is the ease of load balancing since every cell requires the same amount of work resulting in high parallel efficiency. A useful metric for computational cost is the total CPU hours needed for simulation of one flow-through-time (defined as the time needed for a fluid element to pass the length of the combustor (i.e., L/U)). Generally, 7-10 flow-through-times are used requiring 15,000 CPU hours on an IBM Power3-SMP computer. Forty CPU's were used corresponding to approximately 15 days to achieve statistically stationary results. While two weeks may sound like an unreasonable time for engineering applications, this could be greatly reduced by larger processor pools. The use of large, parallel PC clusters has emerged as a viable substitution to traditional high-performance computing (HPC) hardware. As a example of the power of commodity hardware, two PC clusters have been compared to two HPC platforms. A description of the hardware is shown in Table 1. The cost and scalability of the hardware is shown if Figure 1. As can be seen, the PC clusters *Raptor* shows performance comparable to the HPC hardware. With the general trend of doubling processor performance every 18 months, combustor LES on personal or departmental parallel clusters can be completed in a few days in the near future.

For this study, a generic swirling dump combustor is simulated. The geometry consists of a straight inlet duct expanding suddenly into the larger combustion zone. The expansion ratio, D_c / D_i, is 3.2. The inlet length is 1.25 D_i and the combustor is 5.5 D_i. A swirling velocity profile is imparted at the inlet and allowed to evolve towards the dump plane. Downstream, a rapid 60% (D_c / D_e = 2.8) convergence is place in order to accelerate the flow and to excite resonant acoustic modes. It must be noted, however, that the down-stream flow is not choked as is usually the case. A cylindrical grid of 181 × 73 × 81 (axial, radial,

Table 1 Parallel computing hardware comparison. *Owl* and *Raptor* are PC clusters, *Seymour* and *Habu* are specialized high-performance computing platforms.

Name	Platform	SMP Nodes (CPU / node)	CPU Speed (MHz)
Owl	PC-Cluster	4 (4)	500
Raptor	PC-Cluster	12 (2)	733
Seymour	Cray-T3E	1024 (1)	450
Habu	IBM-Power3	334 (4)	375

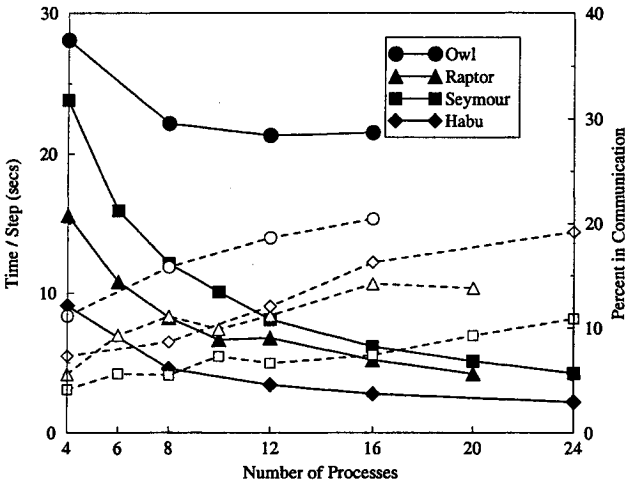

Fig. 1 LES (a) performance and (b) scalability for various parallel computing platforms. In (a), the solid lines/filled symbols represent the total time per step (secs) and dashed lines/filled symbols represent the communication cost (percent of total time).

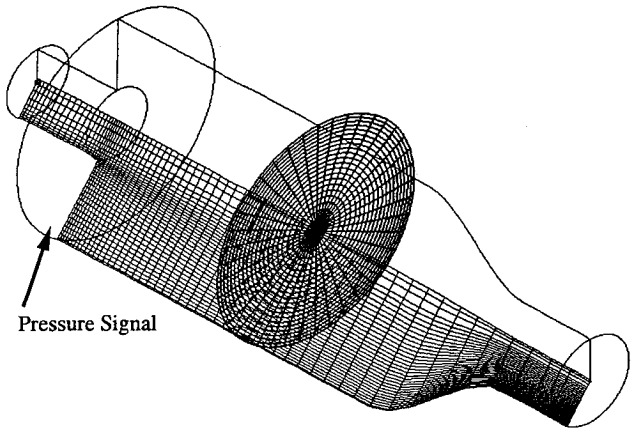

Fig. 2 Geometry and computational grid (181 × 73 × 81) employed in this study (showing only every third grid point). Pressure signal is recorded at the base of the combustor.

azimuthal directions, respectively) is used to discretize the geometry. An isometric view of the computational grid is shown in Figure 2.

The mean inlet mass flow rate, temperature, and pressure are 0.435 Kilograms/second, 673 Kelvin, and 11.8 atmospheres, respectively. The Reynolds number based on the inlet center-line axial velocity and inlet diameter is 527,000. A Gaussian random field (7% of the mean) is added to the inlet velocity profile. The fuel and air at the inflow is assumed to be perfectly premixed. To wash out the effects of the initial conditions the simulations are allowed to evolve several flow-through-times before any data is collected for analysis.

2.1 Premixed Combustion Model

Due to the high expense and numerical difficulties of finite-rate chemistry, the premixed combustion is modeled with a G-equation flamelet formulation following Smith and Menon.[13] In this model, a progress variable G is defined such that $G = 1$ for the reactant gas and $G = 0$ for the products. Upon filtering, the G-equation takes the following form,

$$\frac{\partial \overline{\rho}\tilde{G}}{\partial t} + \nabla \cdot \overline{\rho}\tilde{u}\tilde{G} = -S^{sgs} - \nabla \cdot G^{sgs}, \qquad (1)$$

where $\overline{\rho}$, $\tilde{G}$, $\tilde{u}$ are the filtered density, G, and velocity fields, respectively. The resulting sub-grid terms which require modeling are the unresolved transport, $G^{sgs} = \overline{\rho}[\widetilde{uG} - \tilde{u}\tilde{G}]$, and the source term, $S^{sgs} = \rho_o S_L^o |\nabla G|$. The density and laminar flame speed are both taken at some reference condition. The evolution of the progress variable is balanced by the fluid convection and flame-normal burning rate. Details of the reaction rates and molecular diffusion/conduction are contained in the laminar flame speed, S_L^o. The unresolved transport term is modeled with a gradient diffusion assumption and the source term is approximated as $S^{sgs} \approx \rho_o S_t |\nabla \tilde{G}|$. Here, S_t, is the local turbulent flame speed averaged over a characteristic LES length cell. For the present study, Pocheau's flame speed model[14] has been used to determine the turbulent flame speed in the following form;

$$\frac{S_t}{S_L} = (1 + \beta \frac{u'^{\alpha}}{S_L^{\alpha}})^{\frac{1}{\alpha}}. \qquad (2)$$

Here, $\alpha = 2$ for energy conservation and β is an adjustable parameter set to 20.[8]

Recently, a closure for S_t, known as the *broadened flame model*, has been developed by Kim and Menon[15] which uses dynamically evaluated turbulence quantities (Localized Dynamic K-equation Model, LDKM). This model allows the simulation of flames in the *thin-reaction-zones regime* over a wide range of turbulence levels. We will investigate such a model and its impact on the combustion dynamics in the future.

Table 2 Simulation parameters.

Case ID	Inlet Swirl (S_i)	Equiv. Ratio (Φ)	S_L^o (cm/s)	T_{prod} (K)
1	0.56	0.52	28	1811
2	0.84	0.52	28	1811
3	1.12	0.52	28	1811
4	0.56	0.72	52	2137
5	0.56	0.41	12	1549

3 Results

Five simulations have been conducted with varying degrees of swirl and equivalence ratios in order to investigate their respective effects. A summary of each case is tabulated in Table 2. The inlet velocity profile is given in terms of a Swirl number, S, defined here as:

$$S = \frac{\int_0^R \rho u w r^2 \mathrm{d}r}{R \int_0^R \rho u^2 r \mathrm{d}r}, \qquad (3)$$

where R is the tube radius. The three swirl numbers simulated correspond, approximately, to swirl vane angles of 40°, 50°, and 60°.[5] A variation in Φ is achieved by altering the laminar flame speed, S_L^o, and the product gas temperature, T_{prod}. Chemkin[16,17] was used to calculate S_L^o and T_{prod} for the given methane equivalence ratio. Case 1 is used as the baseline simulation.

3.1 Combustor Aerodynamics

Despite the high swirl imposed at the inlet, the swirl number tends to drop sharply as the flow evolves through the pipe. The resulting swirl numbers at the dump plane (S_d) for cases 1-3 are 0.42, 0.68, and 0.74. The actual swirl numbers through the combustor is

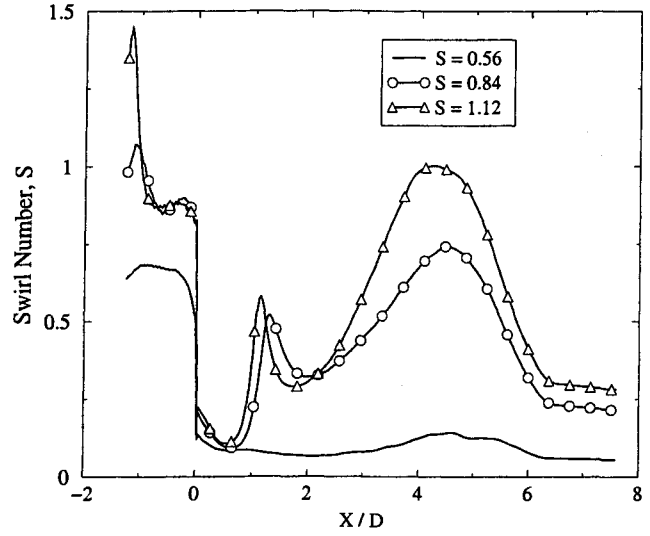

a) $S(x)$

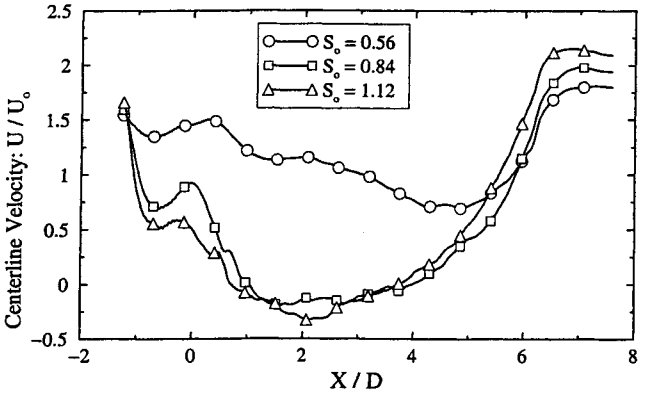

b) $U(x)$

Fig. 3 (a) Mean Swirl number through the combustor. (b) Mean center-line axial velocity ($\overline{U}$ / U_0).

shown Figure 3(a). Examining the mean inlet velocity profiles through the inlet region indicates that the swirl decay rate is proportional to the swirl itself.

As previously stated, swirling flow is often used as a stabilizing mechanism in conjunction with sudden expansions in most combustion devices. For turbulent flows, the critical S at which Vortex-breakdown begins is typically 0.6.[5] Plotted in Figure 3(b) are the mean center-line axial velocity (U_x / U_0) profiles for Cases 1-3. Case 1 exhibited only mild reductions in axial velocity while both Cases 2 and 3 have negative center-line profiles downstream of the dump plane.

To give a better indication of the effects of different swirl on the mean velocity, the radial profiles at various x/D locations are shown in Figures 4-6(a). Only the axial and azimuthal velocities are shown for clarity. Similar to the previous results, Cases 2 and 3 exhibit similar results. The velocity profiles for Case 1 resemble those of a typical jet due to the lower level of swirl. The resulting re-attachment length (δ) for this case is approximately 4 D_i which corresponds to a 3.7 step heights. The subsequent re-attachment lengths for Cases 2 and 3 are δ = 2.1 and 1.4 D_i. As can be seen, the higher levels of swirl greatly increase the spreading rate of the shear layer.

The RMS fluctuations are shown in (b) of Figures 4-6. The most noticeable distinction between the three different simulations is the decrease in axial velocity fluctuations through the inlet. Values of 100% fluctuation are observed for Case 1 but are reduced as the swirl is increased. The high u' values are the result of shear layer instabilities interacting with high-amplitude longitudinal pressure fluctuations. The effects of this on the flame surface will be addressed shortly. As could be expected, high values are seen in the shear layer with correspondingly high levels of anisotropy. Downstream, the flow becomes more uniform and approaches isotropic in the far-field, similar to that observed by Dellenback.[9]

Vortex-breakdown can be seen starting at x / D $\approx$ 1.0 and 0.80 for Cases 2 and 3. Inside the Vortex-breakdown bubble, the axial velocity is negative and the azimuthal velocity is nearly zero. The shape of the breakdown bubble, taken from Figures 5 and 6(c), is toroidal and extends downstream 3 D_i. While the mean velocities are quite low inside the vortex bubbles, the RMS fluctuations remain relatively high.

The impact of Vortex-Breakdown is to give the flame a region of low velocity. Additionally, the RMS fluctuations on the boundary of the vortex-bubble remain relatively high compared to the local mean velocity. The high turbulence intensity increases the turbulent flame speed as governed by Equation 2. The combination of these two effects is to dramatically shorten the flame length. Figure 7 shows the time averaged flame surface for Cases 1-3. The corresponding flame lengths for these cases are 1.73, 0.72, and 0.38 D_i, respectively. The connected flow of Case 1 results in a long, pointed flame similar to that observed for a jet flame. Vortex-Breakdown effects are seen in Cases 2 and 3. There, the pointed flame is not present. Both these flames are broader with a flat head. The end of the flame is located just upstream of the Vortex-Breakdown bubble.

While the tip of the flame surfaces is located at the Vortex-Breakdown bubble, the outer surface is located at the swirling shear layer boundary. Coherent, large-scale vortices are shed at the dump plane due to the previously mentioned shear layer instabilities. These structures are most dominant in the connected flow of Case 1 where they are able to propagate downstream. As a vortex-ring is shed, it entrains the flame surface and draws it downstream before collapsing due to hydrodynamic instabilities. As the swirl is increased, the coherence and stability of these structures decreases

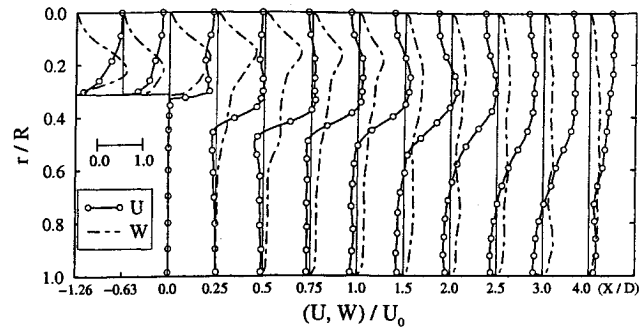

a) $\overline{U}$,$\overline{W}$

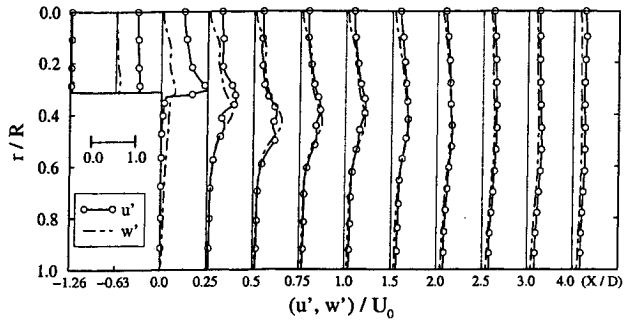

b) u',w'

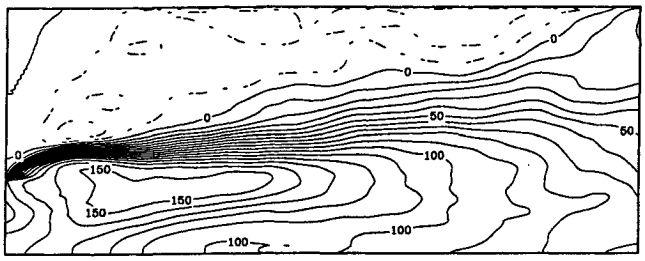

c) $\overline{U}$ Contours

Fig. 4 (a) Mean and (b) RMS radial profiles of U_x (—) and U_θ (- - -) at various x/D locations for Case 1. (c) Mean axial velocity contours from 0 ≤ x / D ≤ 4. Dashed line indicates negative velocity.

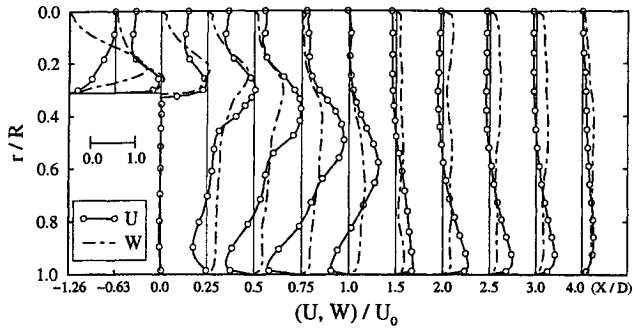

a) $\overline{U}$,$\overline{W}$

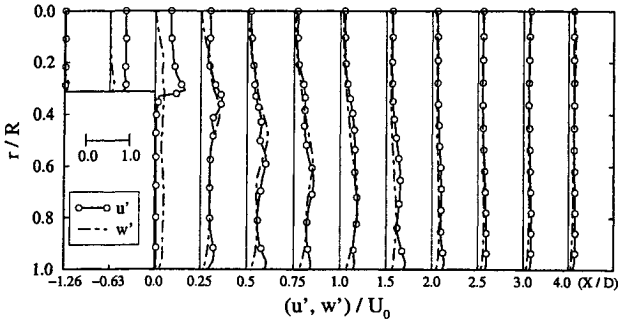

b) u',w'

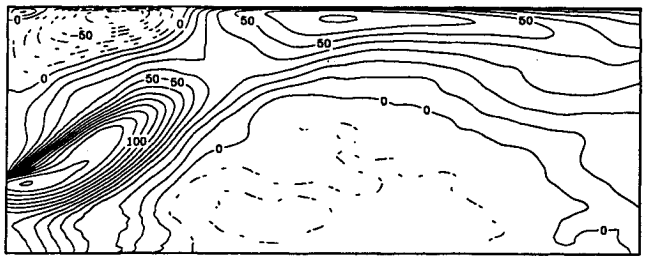

c) $\overline{U}$ Contours

Fig. 5 (a) Mean and (b) RMS radial profiles of U_x (—) and U_θ (- - -) at various x/D locations for Case 2. (c) Mean axial velocity contours from 0 ≤ x / D ≤ 4. Dashed line indicates negative velocity.

with correspondingly less flame entrainment.

3.2 Combustion Dynamics

While the swirling aerodynamics inside the combustion chamber is an interesting field on its own, the impact on combustor stability is of more interest in combustion system design. A key metric on the stability of the combustor is the level of pressure oscillation. The pressure fluctuations were recorded inside the combustor at the location indicated in Figure 2. This location was chosen due to its relatively low vorticity.

The pressure responses to variation in swirl number and equivalence ratio are shown in Figures 8(a) and (b), respectively. As the swirl number is increased, the pressure fluctuations drop. The largest drop in p', by almost 50%, is from $S_i = 0.56$ to $S_i = 0.84$. This drop corresponds to a change of -5.5 dB. As S_i is further increased to 1.12, an additional -1.1 dB drop is achieved. The peak frequency for Cases 1-3 is approximately 3000 Hz with only a small dependence on the initial swirl. An analysis of the Fourier amplitudes at this frequency reveal a 3/4 wave shape with a pressure node occurring slightly downstream of the dump plane.

The strong attenuation in p' occurs when transitioning from to jet-like to re-circulating (i.e., Vortex-Breakdown) flow (Cases 2 and 3).

The analogous p' response to Φ is plotted in Figure 8. Due to the change in T_{prod} and resulting change in sound speed, there is a change in dominant frequency; however, the wavelength of this mode is not been al-

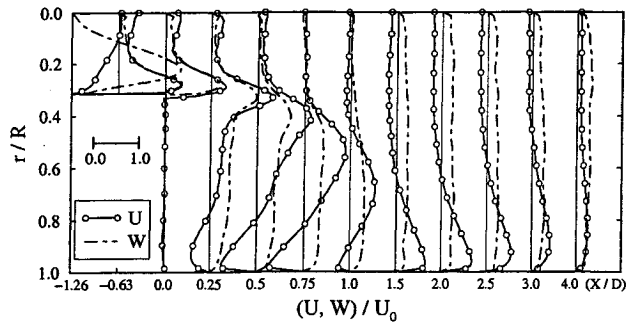

a) $\overline{U}$,$\overline{W}$

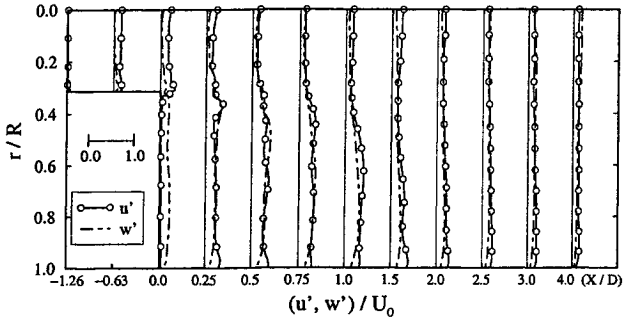

b) u',w'

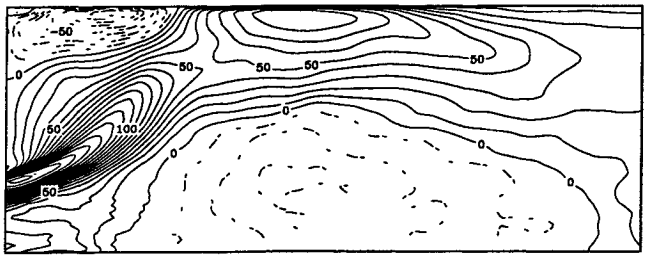

c) $\overline{U}$ Contours

Fig. 6 (a) Mean and (b) RMS radial profiles of U_x (—) and U_θ (- - -) at various x/D locations for Case 3. (c) Mean axial velocity contours from $0 \leq x / D \leq 4$. Dashed line indicates negative velocity.

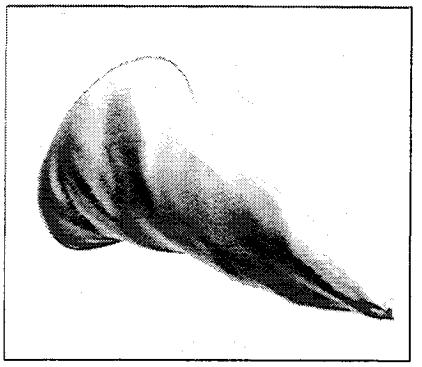

a) $S_i = 0.56$

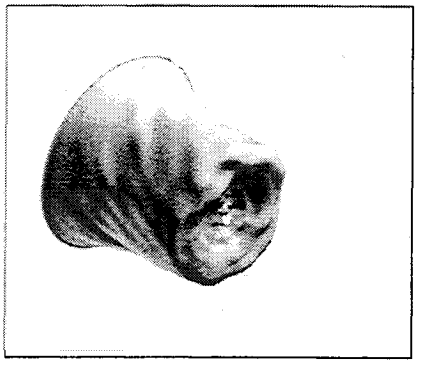

b) $S_i = 0.84$

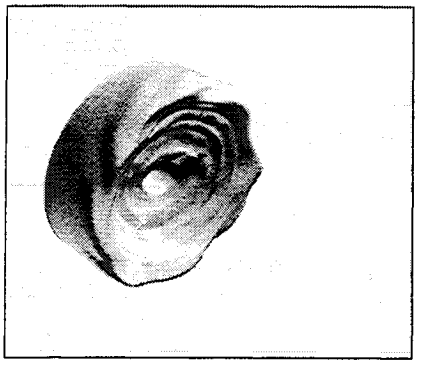

c) $S_i = 1.12$

Fig. 7 Mean flame surface for Cases 1, 2, and 3 with corresponding flame lengths of 1.73, 0.72, 0.38 D_i, respectively. Flow direction is from top left to bottom right. Flame base is at dump plane.

tered. The general trend is an increase in pressure amplitudes in the lean limit. Surprisingly, the leaner burning Case 5 showed a slightly lower fluctuating amplitude (-1.5 dB) as opposed to $\Phi = 0.52$. However, p' did reduce substantially for the richer Case 4. In this case the amplitude was changed by -4 dB.

4 Conclusions

Large-Eddy Simulation methodology has been used to model combustion dynamics in a swirling dump combustor. A G-equation premixed combustion model was used to simulate the flame propagation. The aerodynamic effects of swirl and their resulting effects on flame stability and pressure oscillation have been investigated. It is found that for swirl numbers above a critical value, the center-line axial flow re-circulates or breaks down (i.e., Vortex-Breakdown). Large-scale coherent vortices are observed to shed and entrain the flame at the lowest swirl number resulting in strong pulsation. The coherence and strength of these structures decreased with increasing swirl. Vortex-Breakdown is seen to occur at the higher two swirl numbers. The presence of a stagnated axial flow and high turbulence intensity in the shear layer allows the flame to be more stable. This stability increased with increasing swirl. The increased flame

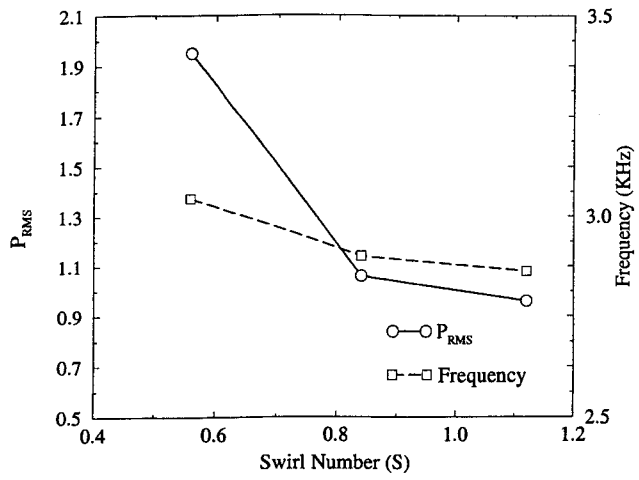

a)

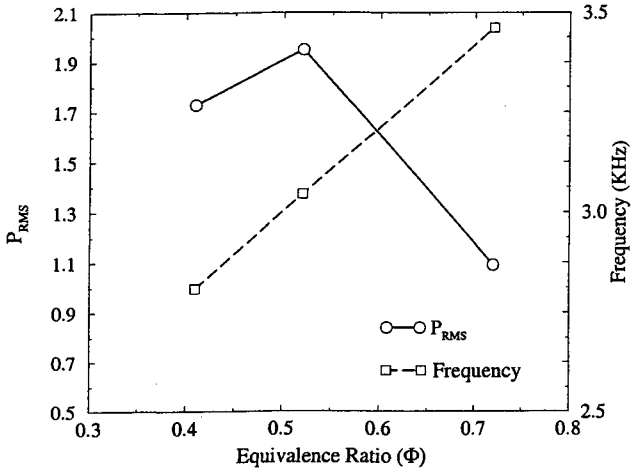

b)

Fig. 8 Response in pressure fluctuations and frequency to changes in (a) Swirl Number (S) and (b) Equivalence Ratio (Φ).

stability resulted in substantial reductions in the fluctuating pressure amplitude. Reductions of 6.6 dB were shown to be possible by changing the swirl vane angle. The impact of equivalence ratio through variations in flame-speed and heat release have also been studied. Results showed that leaner mixtures, those near the Lean-Blowout Limit, exhibited higher amplitude pressure fluctuations.

5 Acknowledgments

This work was financially supported by General Electric Power Systems. High Performance Computing (HPC) resources provided by the Department of Defense (DOD) Major Shared Resources Centers (MSRC) at Naval Oceanographic Office (NAVOCEANO), Aeronautical Systems Center (ASC), and Army Engineering Research and Development Center (ERDC) under Army Research Office (ARO) and Wright-Patterson AFB HPC Grand Challenge Projects.

References

[1] Zinn, B. and Neumeier, Y., "Control of combustion instabilities with secondary fuel injection using real time modes observation: practical implementation," *Proceedings of the Combustion Institute*, Vol. 26, 1996.

[2] Pashereit, C. O., Gutmark, E., and Weisenstein, W. W., "Control of thermoacoustic instabilities and emissions in an industrial-type gas-turbine combustor," *Proceedings of the 27th International Symposium on Combustion*, 1998, pp. 1817–1824.

[3] Pashereit, C. O., Gutmark, E., and Weisenstein, W. W., "Structure and control of thermoacoustic instablities in a gas-turbine combustor," *Combustion Science and Technology*, Vol. 138, 1998, pp. 213–232.

[4] Sivasegaram, S. and Whitelaw, J., "The influence of swirl on oscillations in ducted premixed flames," *Combustion Science and Technology*, Vol. 85, 1991.

[5] Lilley, D. G., "Swirl Flows in Combustion: A Review," *AIAA Journal*, Vol. 15, No. 8, 1977, pp. 1063–1078.

[6] Syred, N. and Beer, J. M., "Combustion in swirling flows: A review," *Combustion and Flame*, Vol. 23, 1974, pp. 143–201.

[7] Paschereit, C., Gutmark, E., and Weisenstein, W. W., "Coherent structures in swirling flows and their role in acoustic combustion control," *Physics of Fluids*, Vol. 11, 1999, pp. 2667–2678.

[8] Kim, W.-W., Menon, S., and Mongia, H. C., "Large eddy simulations of a gas turbine combustor flow," *Combustion Science and Technology*, Vol. 143, 1999, pp. 25–62.

[9] Dellenback, P. A., Metzger, D. E., and Neitzel, G. P., "Measurements in turbulent swirling flow through an abrupt axisymmetric expansion," *AIAA Journal*, Vol. 26, No. 6, 1988, pp. 669–681.

[10] MacCormack, R. W., "The effects of viscosity in hyper-velocity impact cratering," *AIAA Paper 69–354*, 1969.

[11] Menon, S., Sankaran, V., Stone, C., and Sekar, B., "Dynamics of swirling premixed and spray flames," *AIAA-2001-1092*, 2001.

[12] Poinsot, T. and Lele, S., "Boundary conditions for direct simulations of compressible viscous flow," *Journal of Computational Physics*, Vol. 101, 1992, pp. 104–129.

[13] Smith, T. M. and Menon, S., "The structure of premixed flames in a spatially evolving turbulent flow," *Combustion Science and Technology*, Vol. 119, 1996, pp. 77–106.

[14] Pocheau, A., "Scale invariance in turbulent front propagation," *Physical Review E*, Vol. 49, 1994, pp. 1109–1122.

[15] Kim, W.-W. and Menon, S., "Numerical modeling of turbulent premixed flames in the thin-reaction-zones regime," *Combustion Science and Technology*, Vol. 160, 2000, pp. 110–150.

[16] Kee, R. J., Grcar, J. F., Smooke, M. D., and Miller, J. A., "A Fortran program for modeling steady laminar one-dimensional premixed flames," *Sandia Report SAND85-8240, Sandia National Labs., Livermore, CA.*, 1993.

[17] Kee, R. J., Rupley, F. M., and Miller, J. A., "Chemkin-II: A Fortran chemical kinetics package for the analysis of gas phase chemical kinetics," *Sandia Report SAND89-8009B, Sandia National Labs., Livermore, CA.*, 1993.